



Measurement of turbulent dissipation with advanced laser diagnostics

Dr. Peter D. Huck

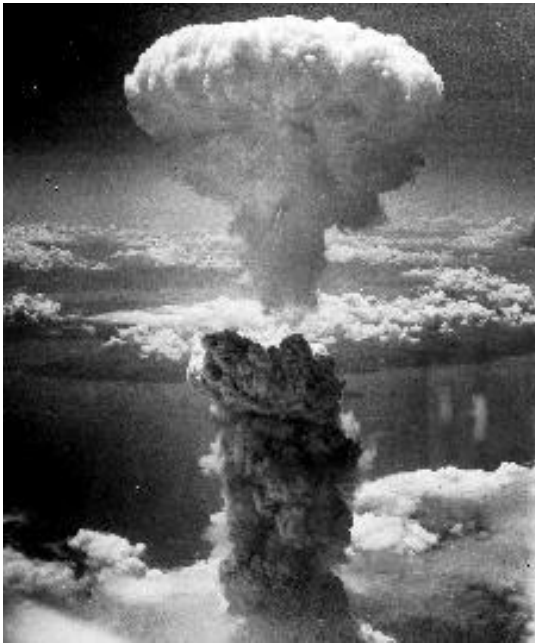
The George Washington University (Prof. Philippe Bardet)

Los Alamos National Lab (Dr. John Charonko)

NSSC3 Kickoff Meeting and Advisory Board Review

April 19-20, 2022

Introduction



Informing numerical models of buoyancy driven flows requires fully resolved velocity gradients and kinetic energy measurements

Department and University: The George Washington University, *Department of Mechanical and Aerospace Engineering*

Academic Advisor: Philippe M. Bardet

NSSC Research Focus Areas: Nuclear Engineering

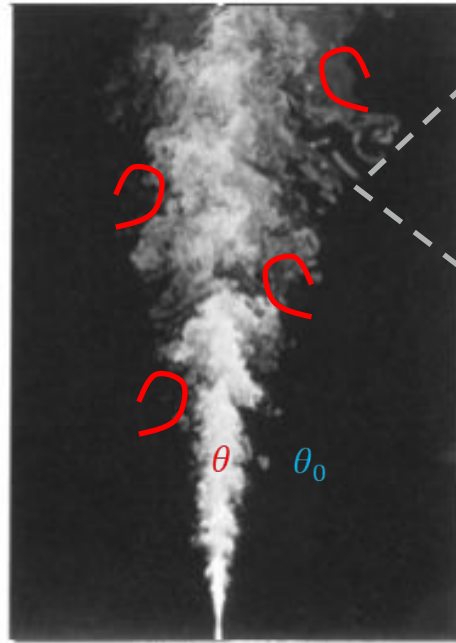
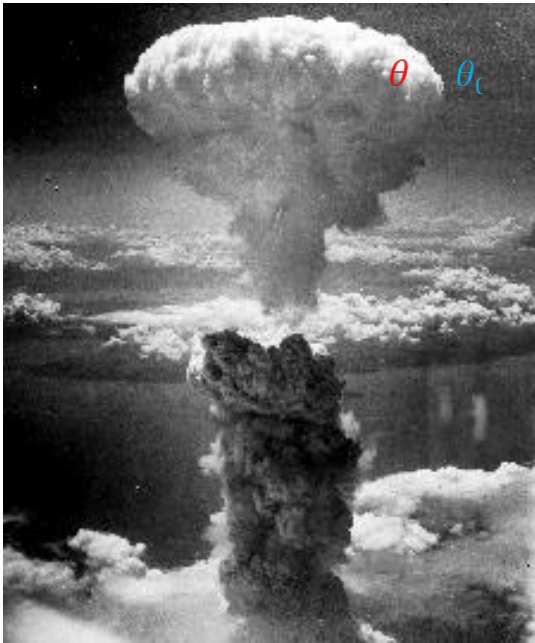
Planned Graduation Date: N/A

Lab Mentor and Partner Laboratory: Dr. John Charonko, LANL

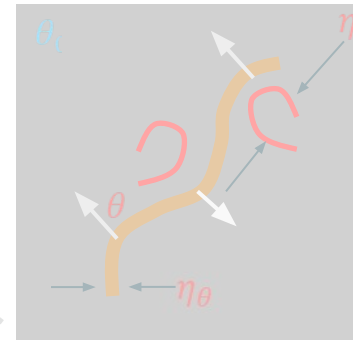
Mission Relevance of Research:

In the case of a global nuclear detonations, detection and disaster mitigation can be accomplished by simulating the rise height and fall out of the resulting buoyant plume. To properly parameterize these simulations, **it is imperative to provide the direct measurement of small scale velocity gradients in a turbulent flow**. This quantity is necessary to determine the rate at which the turbulence dissipates energy and is a fundamental in developing realistic models of turbulent flows. This research supports the NNSA security mission of nuclear detonation forensics by providing CFD models with data inputs with minimal assumptions regarding the resolved scales of the measurement.

Emergency Response to extreme Events



(b) $Re \approx 10^4$



Kolmogorov scale
 $\eta = (\nu^3/\epsilon)^{1/4}$
 Batchelor scale (air)
 $\eta_\theta = \eta Sc^{-3/4}$
 Schmidt number
 $Sc = \nu/D = 0.7$

Mixing occurs when **small-scales** of plume are *similar* to those of turbulence

Strong need for:

- Experimental determination of k & ϵ
- Experimental determination of potential forcing terms in RANS models

prediction efforts begin with a RANS model

Buoyancy contributions to TKE and dissipation

$$\frac{Dk}{Dt} = \mathcal{P}_k + \frac{\partial}{\partial x_j} \left[\left(\nu + \frac{\nu_t}{\sigma_k} \right) \frac{\partial k}{\partial x_j} \right] - \epsilon + \mathcal{F}_k^b$$

$$\frac{D\epsilon}{Dt} = C_{\epsilon 1} \frac{\epsilon P_k}{k} + \frac{\partial}{\partial x_j} \left[\left(\nu + \frac{\nu_t}{\sigma_\epsilon} \right) \frac{\partial \epsilon}{\partial x_j} \right] - C_{\epsilon 2} \frac{\epsilon^2}{k} + \mathcal{F}_\epsilon^b$$

$$\mathcal{F}_k^b = -\rho \beta g_i \overline{u_i \theta}$$

$$\mathcal{F}_\epsilon^b = C_\epsilon \frac{\epsilon}{k} \mathcal{F}_k^b$$

Emergency Response to extreme Events

“The problem of spatial resolution is simply the fact that the sensing element cannot truly respond to scales smaller than its dimensions”

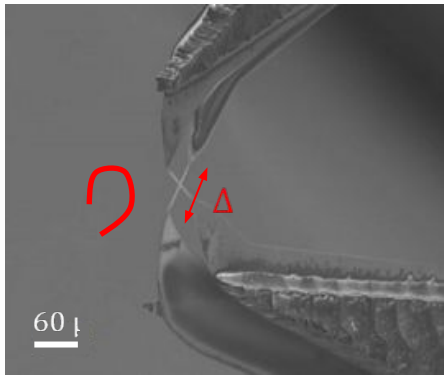
Örlu & Alfredsson, 2010

$$\text{Dissipation rate: } \epsilon = \nu \left\langle \frac{\partial u_i}{\partial x_j} \frac{\partial u_i}{\partial x_j} \right\rangle$$

Deliverables:

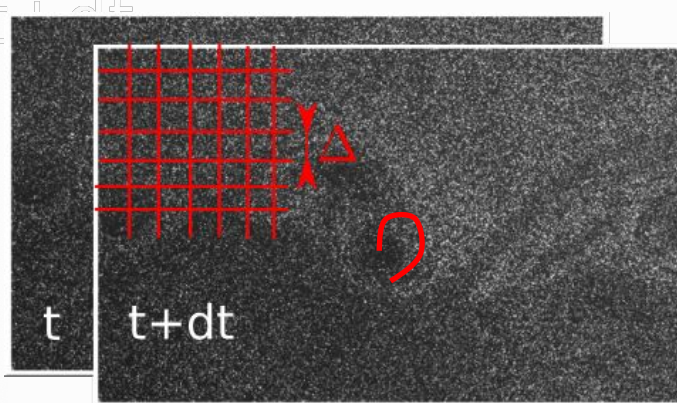
- Develop a compact velocimeter that measures velocity gradients with sufficient resolution to determine ϵ
- Test method in flow configuration where the velocity gradients are known (stagnation point flow)

Hot-wire anemometry



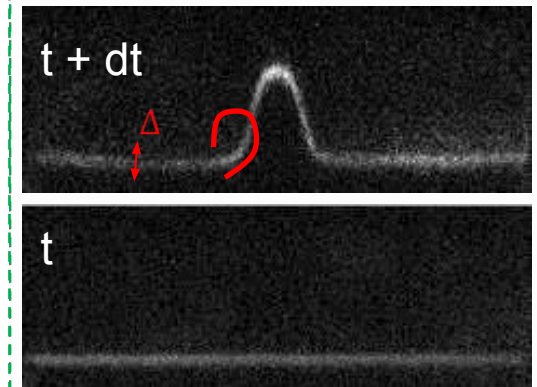
- Spatial filtering of data when wire length $\Delta/\eta \gg 1$
- Indirect measurement velocity gradient

PIV



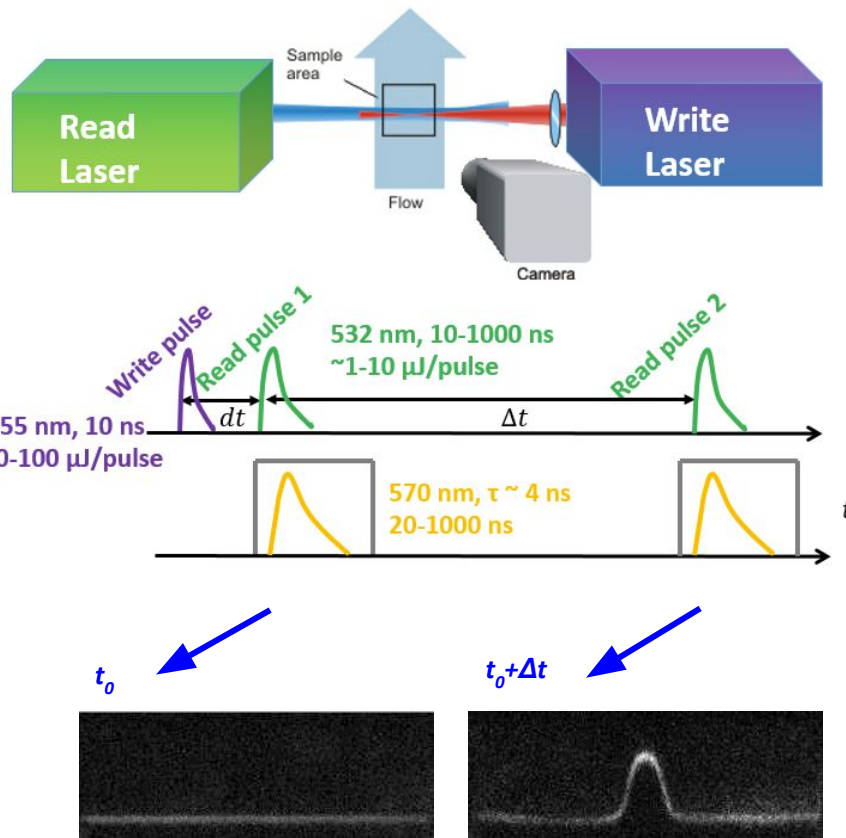
- Interrogation window (Δ) limits resolution of velocity derivative
- Velocity gradient amplifies noise in the dissipation measurement

MTV



- Beamlet width (Δ) limits resolution of probe
- Velocity derivative encoded in the time of flight measurement

Microscopic Molecular Tagging Velocimetry (μ -MTV)



Operating Principles of μ -MTV

- **Spectroscopy** of molecular tracers (seeded or naturally present)
- **Tracer activation** (tagging) with a first laser (**write**)
- **Time of flight** of tagged pattern with a 2nd laser (**read**)

Spectroscopic determination of thermodynamic state variables:

- **Pressure** (in gas) : *Basu et. al., Exp. Fluids (2010)*
- **Temperature** (in gas) : *Matthew et. al., AIAA (2015)*
- **Temperature** (in liquid) : *Natrajan and Christensen, Meas. Sci. Technol. 2009*

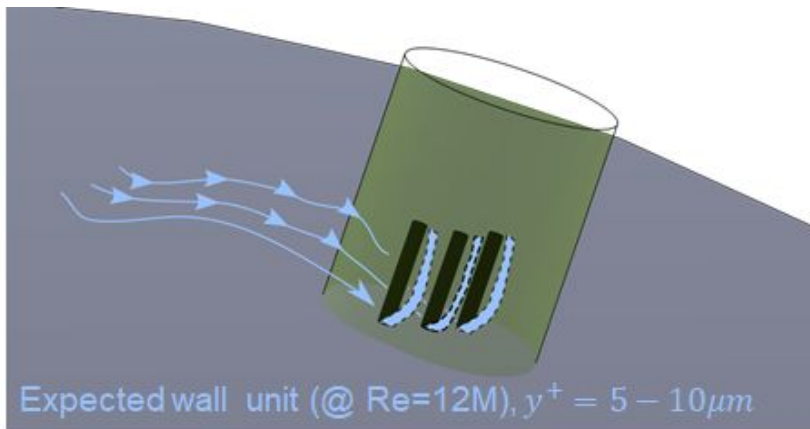
Simultaneous Concentration/Velocity

Temperature/Velocity measurements :

Koochesfahani et. al. Meas. Sci. Technol. 2000

Structured Illumination gives a uniform pattern along the optical axis

Goal: Instantaneous 3D-2C
Velocity measurements at
a solid interface



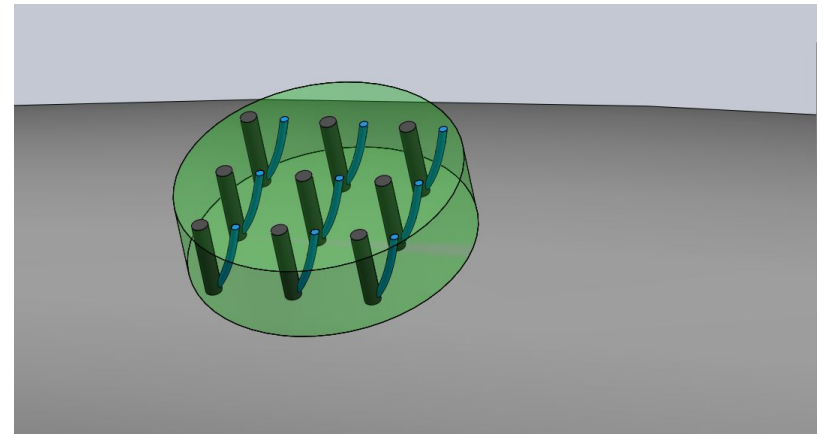
Tagged pattern (black) is deformed (blue) by the fluid flow

Talbot Effect Structured Illumination

Fort et al., *Exp Fluids* (2020a)

$$z_T = 254 \text{ mm}$$

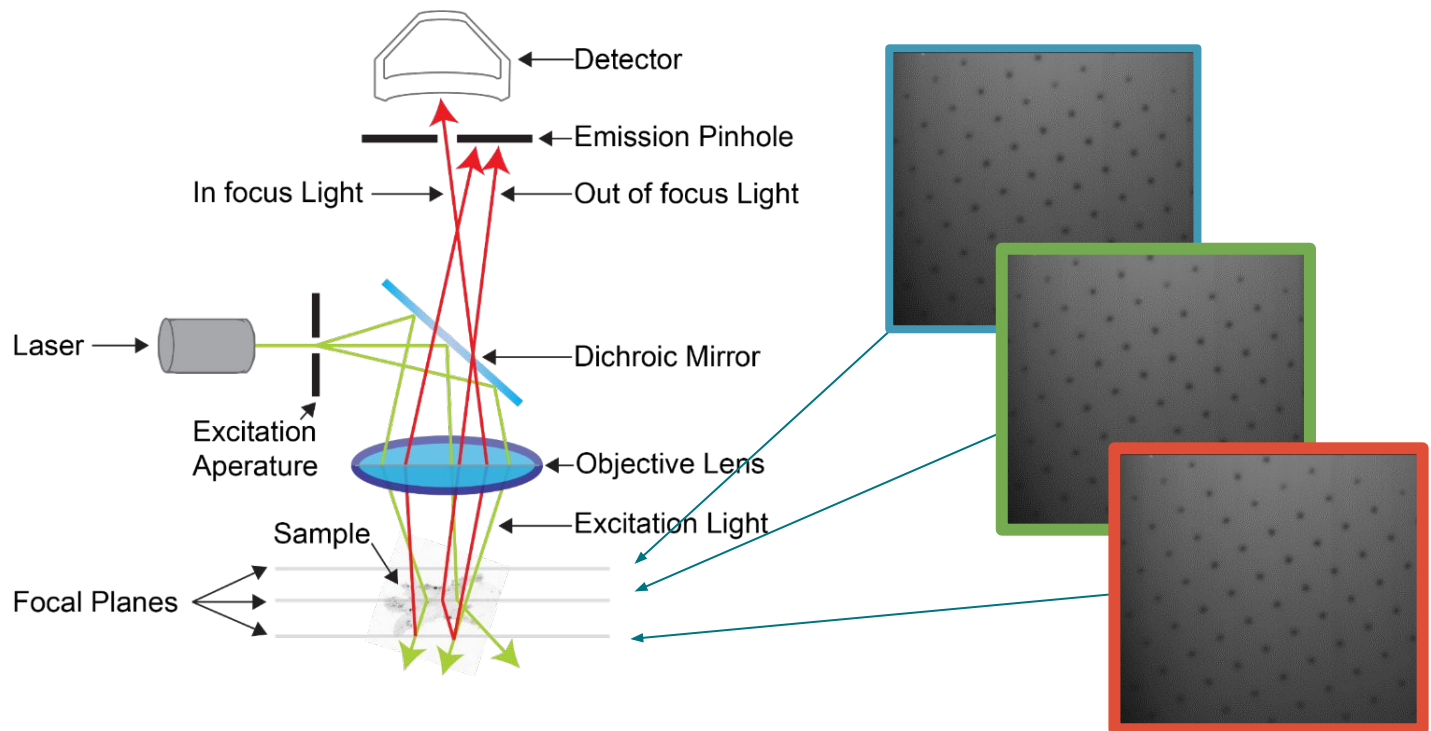
$$p = 300 \mu m, w = 33 \mu m$$



Optical sectioning provides in focus images at different depths

Principle of Microscopic Integral Velocimetry (MIV)

Confocal Microscopy: “Emission Pinhole” permits fine optical sectioning at focal planes



Velocimetry (μ PIV, Shake The Box)

2 Camera Microscopy & Velocimetry

Kim et. al., Exp. Fluids (2011)

Resolution: $R_{xy} = 32 \mu\text{m}$

6 Camera Tomography – 4D PTV “Shake the Box”

Schroöder et. al., Flow Turbulence Combust (2015)

Resolution: $R_{xy} = 93 \mu\text{m}$

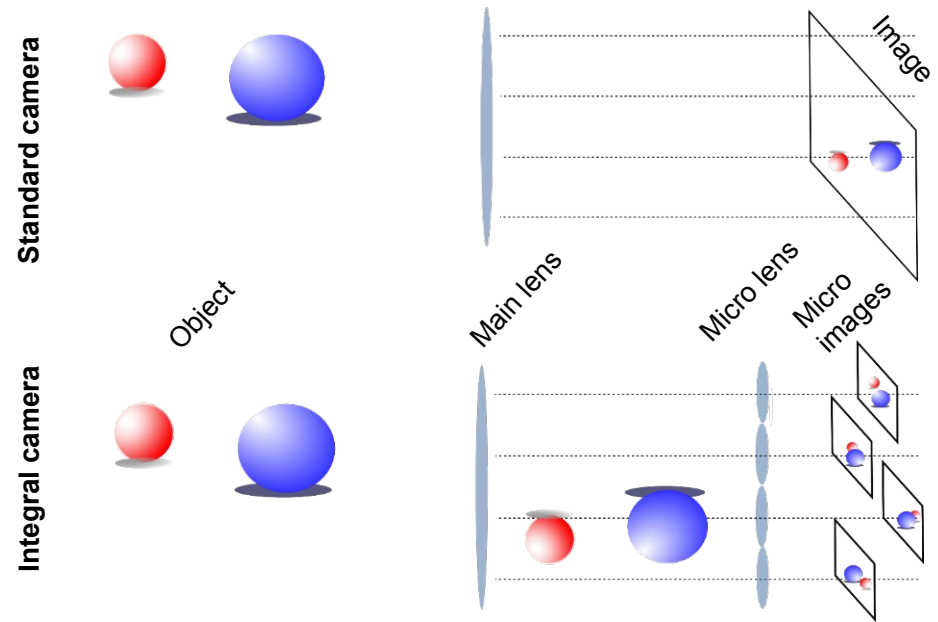
Operational Principles of Integral Imaging

Levoy (2005)



Applications

- Optical aberration, temperature, and density variation characterization
Clifford et. al. , AIAA (2017)
Wilson, Mon. Not. R. Astron. (2002)
- Sensor fusion – synthetic aperture:
Levoy et al. ACM Trans. (2004)
- Optically assisted surgery:
Le et. al., Chin. Opt. Lett (2017)



Design Tradeoffs:

Reduce spatial resolution
Increased angular resolution

Microscopic Integral Velocimetry (MIV) Resolution

Design Criteria

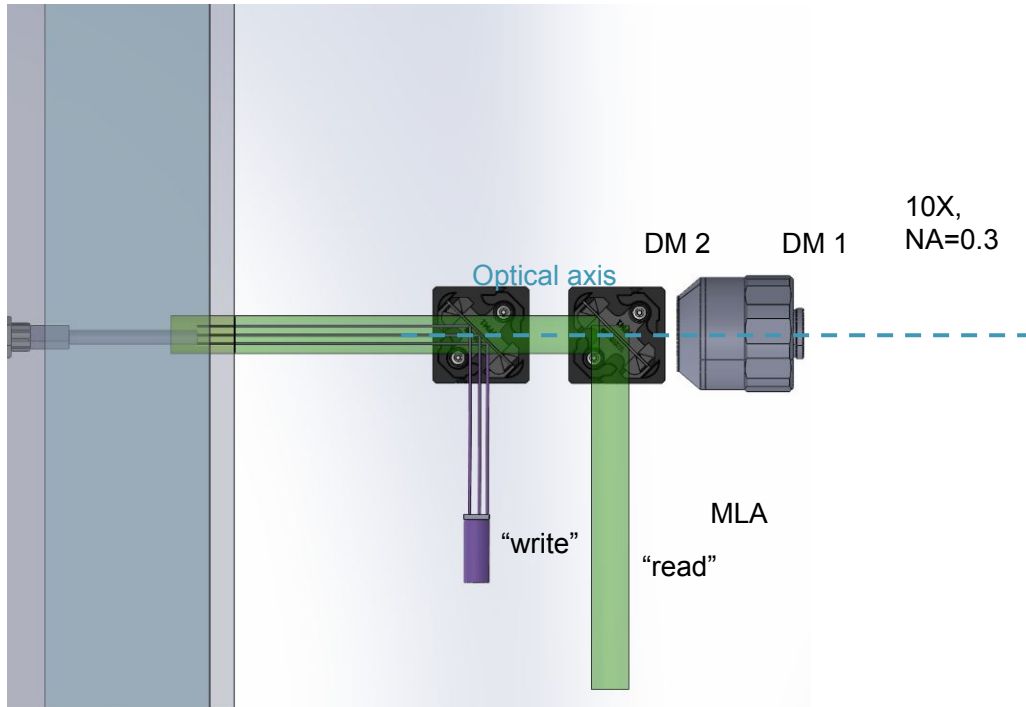
$l_v(\mu\text{m}) \in [5, 11]$: viscous length scales

$t_v(\mu\text{s}) \in [25, 120]$: viscous temporal scales

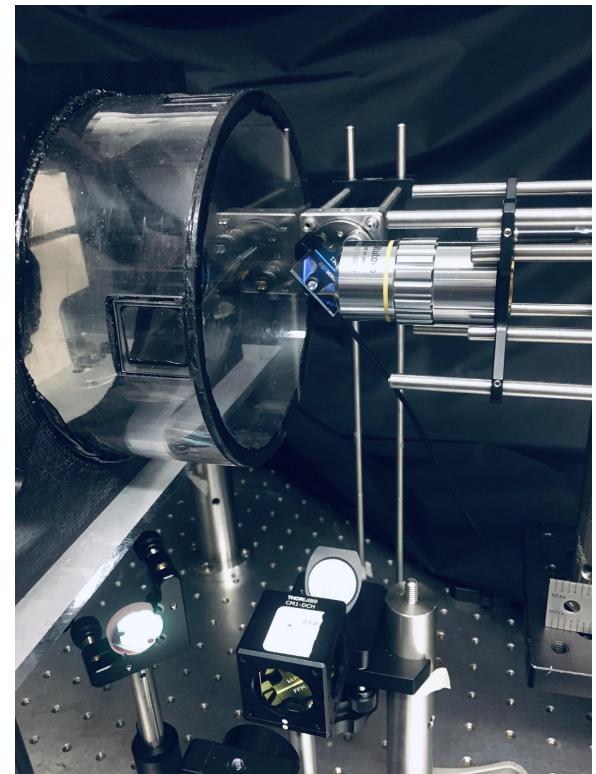
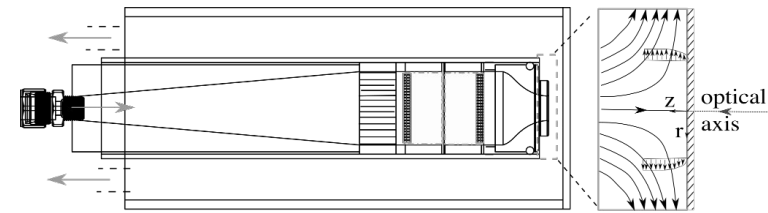
$f_s(\text{kHz}) = 2(t_v)^{-1}$: sampling frequency $\in [16, 80]$ kHz

type			
Confocal M=20X NA=0.4			
FIMic M=20X NA=0.4			

Optical implementation in a newly designed facility



Stagnation Jet Facility



Validate Schlichting Theory for Axisymmetric Stagnation Jet

Similarity Solution $f''' + 2ff'' + 1 - f'^2 = 0$

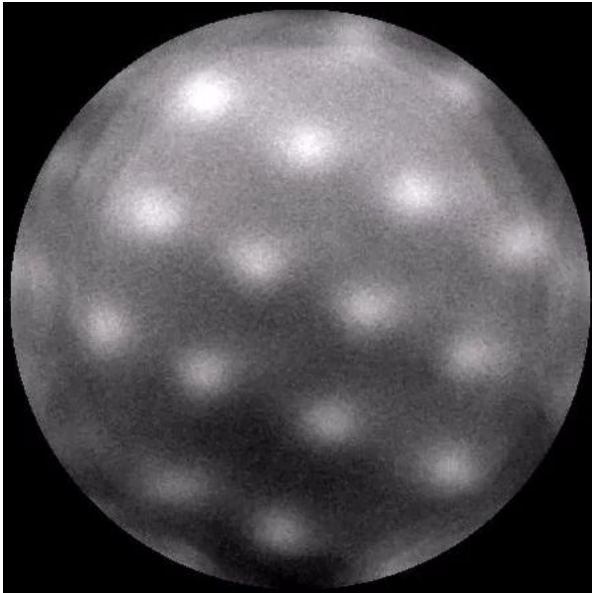
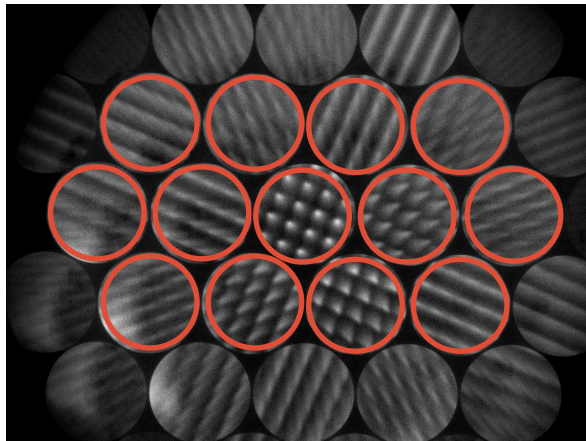
Velocity Profile $u/(\alpha r) = f'(\eta)$

Validate Prediction for Boundary Layer Thickness

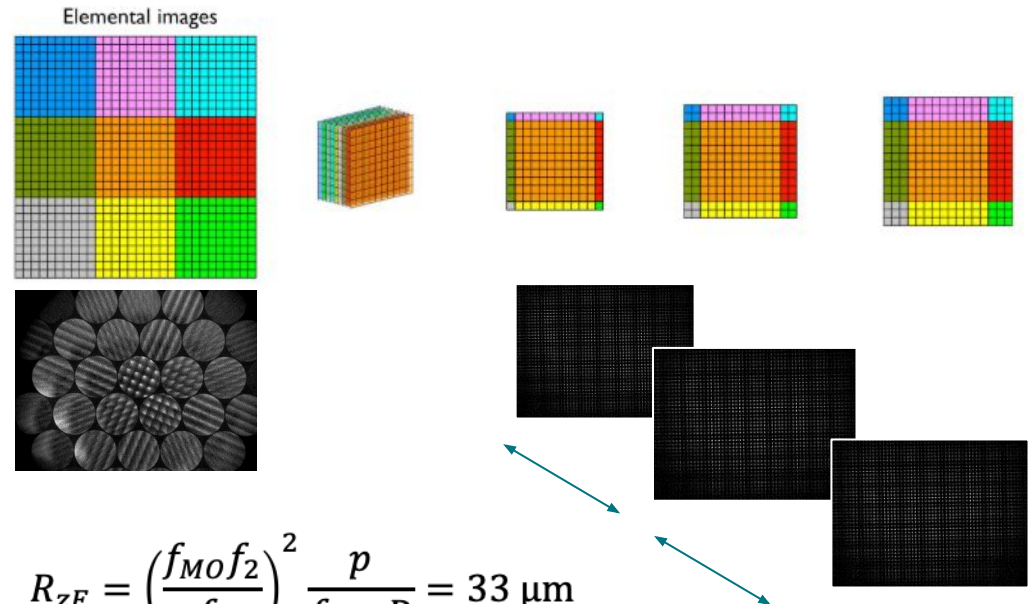
Boundary Layer Height $\delta = 2.8\sqrt{\nu/\alpha}$.

Raw (background subtracted/inverted) images

13 “mini cameras”



Back projection of EIs into physical space (& sum)

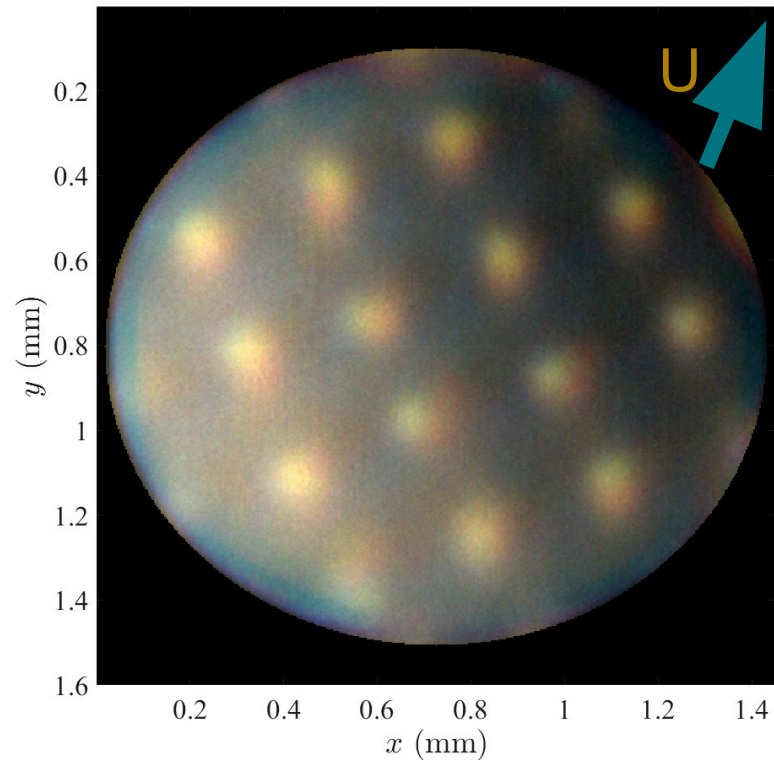
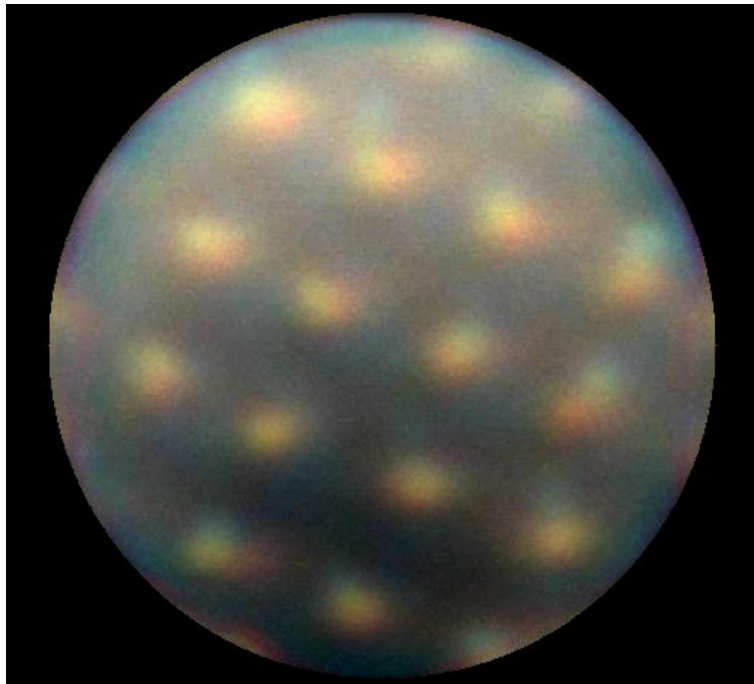


$$R_{ZF} = \left(\frac{f_{Mof2}}{f_1} \right)^2 \frac{p}{f_{MLA}D} = 33 \mu\text{m}$$

(10X , NA=0.28)

First approach to rendering

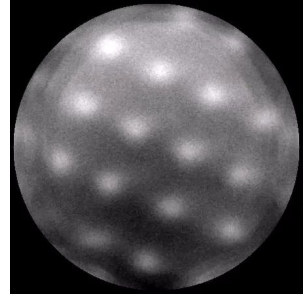
$t = 70 \mu\text{s}$



Theoretical Depth of Field $\Delta_{ZF} = 260\mu\text{m}$
Theoretical Axial Resolution $R_{ZF} = 33\mu\text{m}$

3D-2C Instantaneous Velocimetry

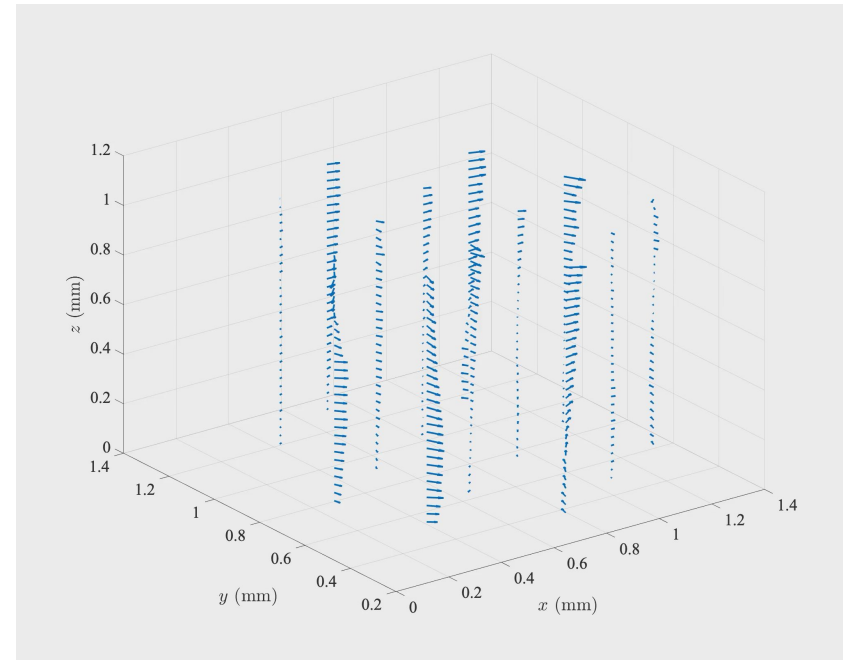
- Vertical resolution ($33 \mu\text{m}$), smooth gradients
- Lateral resolution ($300 \mu\text{m}$), probe
- Probe resolution ($30 \mu\text{m}$)
- 3D structures apparent



Huck et. al. , NURETH 19, 2022.

Huck et. al., International Symposium on Applications of Laser and Imaging Techniques to Fluid Mechanics Lisbon, 11-14 July 2022

Huck et. al. , Symposium Naval Hydrodynamics 2022.



The NSSC Experience

NSSC involvement has broadened my scientific culture and opened up doors professionally.

- "Non-destructive testing". NSSC conference series, Dr. Steve Glenn, LLNL.

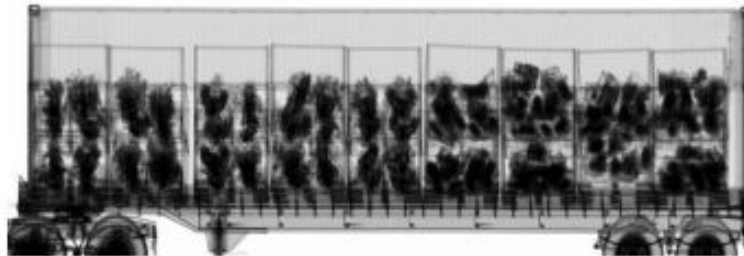
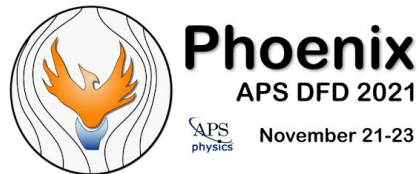


Fig. 3. Example cargo radiograph from a Smiths Detection HCVP NII system.

*Martz et. al., IEEE
Transactions Nuclear
Science, 2016*

- Networking and gained understanding of role of hydrodynamics in National Laboratory Research



- Under consideration for "Experimental Physicist Position", Lawrence Livermore National Lab



Acknowledgements

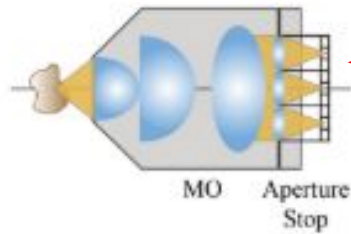


This material is based upon work supported by the Department of Energy National Nuclear Security Administration under Award Number **DE-NA0003996**.

This presentation was prepared as an account of work sponsored by an agency of the United States Government. Neither the United States Government nor any agency thereof, nor any of their employees, makes any warranty, express or implied, or assumes any legal liability or responsibility for the accuracy, completeness, or usefulness of any information, apparatus, product, or process disclosed, or represents that its use would not infringe privately owned rights. Reference herein to any specific commercial product, process, or service by trade name, trademark, manufacturer, or otherwise does not necessarily constitute or imply its endorsement, recommendation, or favoring by the United States Government or any agency thereof. The views and opinions of authors expressed herein do not necessarily state or reflect those of the United States Government or any agency thereof.

The geometry of Fourier Integral Microscopy (FIMic)

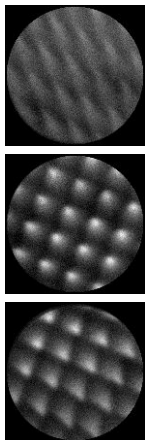
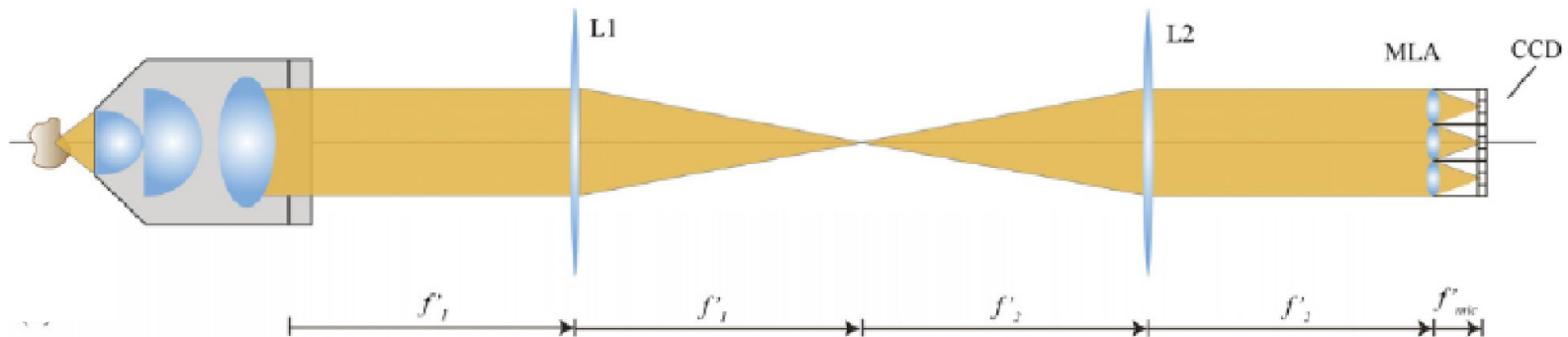
Principle



N microlenses (in diagonal) subsample the aperture (of Fourier) plane of the microscope objective

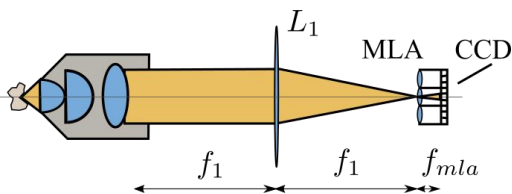
$$NA_{FIMic} = \frac{NA_{MO}}{N}$$

Practical implementation



Three approaches to Integral Microscopy

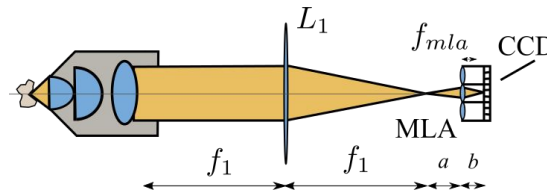
Plenoptic 1.0



- High angular (depth) resolution
- Low spatial (lateral) resolution

Plenoptic 2.0

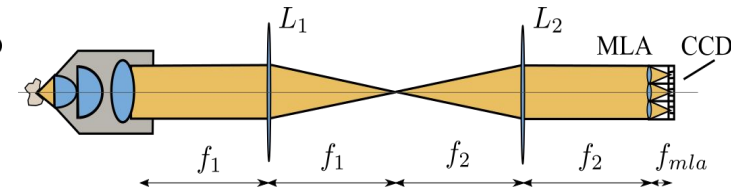
Huck et. al. , NURETH 19, 2022.



- High spatial resolution
- Extended depth of field
- Long Working Distance
- Low angular resolution
- Black box post-processing
- High Resolution (>25MP) cameras (low acquisition rate)

Fourier Integral Microscopy - FIMic

Huck et. al. , Provisional Patent - Wall Shear Stress Optical Probe, 2022.



- Higher spatial resolution
- Flexible design and operation. Active community (open source)
- Modest Resolution (~5-16MP) cameras (high acquisition rate)
- Restricted depth of Field. Small working distance

Talbot-effect structured illumination (TESI) generates fine and flexible laser patterns

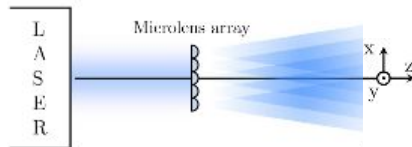
Structured Illumination: **intensity modulation** of excitation light in the spatial domain.

Device	Reference	p (mm)	w (mm)
Beam blockers	Roetmann et. al. (2008)	0.48	0.16
Ronchi gratings	Charogiannis et. al. (2019)	0.2	0.1
Beam Dividers	Chu and Liao (1992)	2	0.15
Micro lens array	Sheng et. al. (2017)	0.5	0.3
Talbot Effect	Fort et. al. (2020)	0.038	0.017

Further uses:

- Sub probe-volume resolution in LDV :
Konig et. al. , Meas. Sci. Technol. (2017)
- Vibration monitoring and profilometry :
Agarwal et. al., Opt. Eng. (2018)
Spagnolo et. al., J. Opt. A. Pure Appl. Opt. (2002)
- Extreme UV Lithography :
Isoyan et. al., J. Vac. Sci. Technol. , (2009)

TESI: **Interferometric** technique for flexible Creation of small-scale patterns



Talbot distance:

$$z_T = \frac{p_0^2}{\lambda}$$

Pattern periodicity varies along z

$$p \left(z = \frac{M}{N} z_T \right) = \frac{p_0}{N}$$

